Author Manuscript

Author Manuscript

Author Manuscript

Author Manuscript

HHS Public Access

Author manuscript

J Proteome Res. Author manuscript; available in PMC 2018 August 04.

Published in final edited form as:

J Proteome Res. 2017 August 04; 16(8): 2983–2992. doi:10.1021/acs.jproteome.7b00275.

Selective affinity enrichment of nitrotyrosine-containing peptides for quantitative analysis in complex samples

Yingxin Zhao[1,2,3,*], **Yueqing Zhang**[1], **Hong Sun**[1], **Rosario Maroto**[2,3], and **Allan R Brasier**[1,2,3]

[1]Department of Internal Medicine, University of Texas Medical Branch (UTMB), Galveston, TX

[2]Institute for Translational Sciences, UTMB, Galveston, TX

[3]Sealy Center for Molecular Medicine, UTMB, Galveston, TX

Abstract

Protein tyrosine nitration by oxidative and nitrate stress is important in the pathogenesis of many inflammatory or aging-related diseases. Mass spectrometry analysis of protein nitrotyrosine is very challenging because the non-nitrated peptides suppress the signals of the low-abundance nitrotyrosine (NT) peptides. No validated methods for enrichment of NT-peptides are currently available. Here we report an immunoaffinity enrichment of NT-peptides for proteomics analysis. The effectiveness of this approach was evaluated using nitrated protein standards and whole-cell lysates *in vitro*. A total of 1,881 NT sites were identified from a nitrated whole-cell extract, indicating that this immunoaffinity-MS method is a valid approach for the enrichment of NT-peptides, and provides a significant advance for characterizing the nitrotyrosine proteome. We noted that this method had higher affinity to peptides with N-terminal nitrotyrosine relative to peptides with other nitrotyrosine locations, which raises the need for future study to develop a pan-specific nitrotyrosine antibody for unbiased, proteome-wide analysis of tyrosine nitration. We applied this method to quantify the changes in protein tyrosine nitration in mouse lungs after intranasal poly(I:C) treatment and quantified 237 NT sites. This result indicates that the immunoaffinity-MS method can be used for quantitative analysis of protein nitrotyrosines in complex samples.

Table of Contents Graphic

[*]Correspondence and requests for reprints should be addressed to: Yingxin Zhao, Ph.D., MRB8.138, University of Texas Medical Branch, 301 University Blvd., Galveston, TX 77555-1060, Phone: 409-772-1923, Fax: 409-772-8709, yizhao@utmb.edu.

Conflict of interest disclosure

The authors declare no competing financial interests.

Author Manuscript Author Manuscript Author Manuscript Author Manuscript

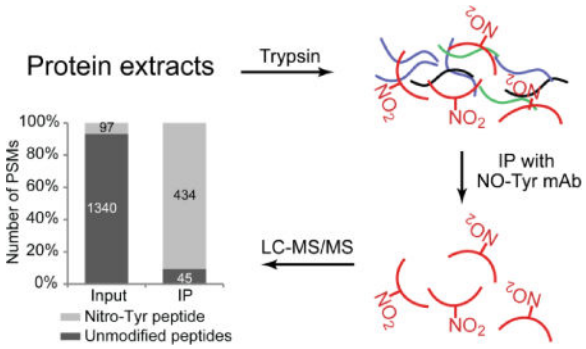

Keywords

Protein tyrosine nitration; Mass spectrometry; Posttranslational modifications; Affinity enrichment

INTRODUCTION

Tyrosine nitration of proteins occurs under conditions of oxidative and nitrative stress where reactive nitrogen species (RNS) such as peroxynitrate ($ONOO^-$) or nitric oxide (·NO) are generated. RNS react with tyrosine residues at the ortho-position relative to the phenolic hydroxyl group, causing nonenzymatic protein tyrosine nitration. Protein tyrosine nitration is a prominent protein posttranslational modification thought to be important in the pathogenesis of severe asthma,[1,2] neurodegenerative disorders,[3,4] atherosclerosis,[5,6] diabetes,[7] cancer,[8] and normal biological aging.[9,10] Tyrosine nitration can alter the protein structure and function, leading to the loss of enzyme or receptor activities.[11–14] Moreover, tyrosine nitration may interfere directly or indirectly with phosphorylation of tyrosine residues important for signaling pathways.[15]

To understand the biological impact of tyrosine nitration and elucidate its roles in signal transduction, the protein targets and precise locations of tyrosine nitration must be known. Various MS-based approaches have been used to identify NT-containing proteins and locate the sites of tyrosine nitration.[9,16,17] A common approach is two-dimensional polyacrylamide gel electrophoresis, followed by Western blotting with antibodies against 3-nitrotyrosine and protein identification via mass spectrometry (MS).[18–20] However, unambiguous identification of proteins and localization of the sites of NT modifications is difficult to achieve by this approach because multiple proteins are usually identified from a single gel spot, and NT sites are rarely identified.[21,22] In addition, the cross-reactivity of antibodies may further compromise the certainty of identification of NT-containing proteins.[23] System-wide analysis of tyrosine nitration via a shotgun proteomic approach is very challenging because the endogenous nitration levels in biological samples are extremely low.[24,25] The detection of NT-containing peptides is obscured by the signals of the non-nitrated peptides, which overwhelm those of the nitrated peptides. For this reason, a specific enrichment approach for nitrotyrosine- containing tryptic peptides prior to MS analysis would be valuable. Several methods using chemical derivatization of 3-nitrotyrosine followed by affinity enrichment have been developed with modest sucess.[26–29] Several limitations of chemical derivatization methods have been well documented. First, these methods usually

Author Manuscript Author Manuscript Author Manuscript Author Manuscript

involve multi-step derivatization protocols, so sample losses during derivatization and cleaning are inevitable.[30,31] Second, the low yield of the chemical reactions and nonspecific derivatization to other amino acid residues compromise the recovery of NT-containing peptides.[30,31] Finally, the affinity tags that are introduced into tryptic NT peptides complicate MS/MS fragmentation, making peptide identifications ambiguous.[31,32] Indeed, only a modest number of NT sites (30–250) were identified from *in vitro* nitrated samples using these approaches.[26–29] For these reasons, we sought a method that enables direct analysis without prior chemical derivatization.

A previous approach using immunoaffinity enrichment of NT peptides used a monoclonal antibody (mAb) (MAB5404, was produced using nitrated KLH as an immunogen) but only two NT sites were identified.[33] The poor success may due to the lack of selectivity and low efficiency of the mAb used in the study.[29] Here, we report and validate an approach for proteomic analysis of protein tyrosine nitration that combines immunoaffinity purification of NT-containing peptides and unambiguous identification of NT sites using a high-accuracy mass spectrometer. The NT-containing peptides were enriched with a different anti-3-nitrotyrosine mAb that shows high specificity for NT peptides.[34,35] The effectiveness of this approach for identifying NT sites and NT-containing proteins was evaluated using standard protein and *in vitro* nitrated whole-cell lysates. A total of 1,559 unique NT peptides, 1,881 NT sites and 907 nitrotyrosine proteins were identified in a cell extract nitrated *in vitro*, indicating that this novel immunoaffinity-based method is a valid approach for enrichment of nitrotyrosine peptides and provides a significant advance for characterizing the nitrotyrosine proteome. We further applied this approach to quantify the changes in protein tyrosine nitration in mouse lungs in response to intranasal poly(I:C) treatment. A total of 147 NT peptides and 237 NT sites was quantified, with 14 nitrotyrosine sites significantly upregulated by poly(I:C) treatment, indicating that this immunoaffinity-MS method can be used for the quantitative analysis of nitrotyrosine in complex samples.

EXPERIMENTAL PROCEDURES

Chemicals and Materials

Nitrated bovine serum albumin (BSA), polyinosinic–polycytidylic acid (poly(I:C) and all chemicals, unless specified otherwise, were from Sigma-Aldrich (St. Louis, MO). Peroxynitrite was from Calbiochem (San Diego, CA). HPLC-MS grade H_2O, methanol, acetonitrile, formic acid and trifluoroacetic acid were from Fisher Scientific (Waltham, MA). Sequencing grade modified trypsin was from Promega (Madison, WI). Anti-nitrotyrosine antibody (clone 39B6) and Protein A/G PLUS-Agarose beads were from Santa Cruz Biotechnology (Dallas, TX), Inc. Biotin-conjugated nitrotyrosine antibody was from Novus Biologicals (Littleton, CO). Nanolink Streptavidin magnetic beads were from Solulink (San Diego, CA).

In vitro nitration of standard protein and cell extract

Bovine serum albumin (10 mg/mL) in 50 mM NH_4HCO_3 (pH7.8) was treated with 20 mM peroxynitrite. After quick vortexing, the sample was incubated for 20 min on ice and 100 mM dithiothreitol (DTT) was then added to quench the reaction.

Author Manuscript Author Manuscript Author Manuscript Author Manuscript

Human alveolar adenocarcinoma cells (A549) were cultured as monolayers in F12K media with 10% fetal bovine serum, penicillin (100 U/ml) and streptomycin (100 μg/ml) at 37°C in a 5% CO_2 atmosphere [36,37]. Plates were washed three times with phosphate-buffered saline (PBS) before harvesting by scraping. The cells were collected, transferred to conical tubes, pelleted at 150Xg for 4 min and resuspended in 1.0 mL of Trizol reagent (Invitrogen, Carlsbad, CA).. The cells were lysed thoroughly by repetitive pipetting. The proteins, which are free of nucleic acids, were extracted from this cell lysate using Trizol reagent per the manufacturer's instructions. The protein pellet was resuspended in 50 μL of 8 M Guanidine HCl and the protein concentration measured by Bradford assay. One milligram of protein was used for *in vitro* nitration: An aliquot of 20 μL of 20 mM peroxynitrite was added to the sample; after quick vortexing, the sample was incubated for 20 min on ice and 50 μL of 100 mM DTT was then added to quench the reaction.

Animal protocols and lung tissue collection

Male mice (strain C57BL/6J, 8–10 weeks old, 25–30 g) were purchased from Jackson Laboratory (Bar Harbor, ME) and housed according to UTMB IACUC protocol # 1312058. For poly(I:C) treatment, mice (6 per experimental group) were lightly anesthetized. A freshly prepared solution of poly(I:C) in PBS (300 μg/ 40 μL) was administered slowly via the intranasal route, alternating nostrils. Twenty-four h later, mice were anesthetized (ketamine/xylazine; 70/10 mg/kg i.p.), anti-coagulated (5 units heparin), then exsanguinated prior to rapid aortic perfusion with ice-cold PBS to quickly rinse the lungs free of blood. The lungs were collected and stored at −80°C until being processed for protein extraction. Controls were mice administered the same volume of PBS i.n.

Tissue processing and protein extraction

For each mouse, about 100 mg of lung tissue was homogenized in 200 μL of ice-cold PBS with a tissue homogenizer. About 1 mL of Trizol® reagent (Invitrogen, Carlsbad, CA) was added to the homogenate. The proteins were extracted from the lysate per the manufacturer's instructions. The proteins were precipitated with isopropanol. The protein pellet was dissolved into 8 M guanidine hydrochloride.

Trypsin digestion

The proteins were first reduced with 10 mM DTT at room temperature for 30 min, followed by alkylation with 30 mM iodoacetamide at room temperature for 2 h. The sample was then diluted with 50 μL of 50 mM ammonium bicarbonate (pH 8.0). An aliquot of Lys-C/Trypsin solution (Promega, Madison, WI) was added to each sample at a 100:1 protein: enzyme ratio. The samples were incubated at 37 °C for overnight, and the solutions further diluted with 400 μL of 50 mM ammonium bicarbonate (pH 8.0). An aliquot of trypsin solution (Promega, Madison, WI) was added to each sample at a 50:1 protein: enzyme ratio. The samples were incubated at 37 °C for 16 h, when 10 μL of 10% trifluoroacetic acid was added to each sample to stop digestion. Tryptic peptides were desalted on reversed-phase tC18 Sep-Pak columns (Waters, Milford, MA) and evaporated to dryness in a vacuum concentrator.

Author Manuscript Author Manuscript Author Manuscript Author Manuscript

Affinity enrichment of nitrotyrosine-containing peptides

The peptides derived from 1 mg of proteins were resuspended in 50 μL of binding buffer (50 mM Tris HCl [pH 8.0], 100 mM NaCl, 1 mM EDTA, 0.5% NP40), and 40 μL of anti-nitrotyrosine antibody (clone 39B6) (100μg/mL) was added to the sample for an overnight incubation at 4°C with gentle rotation; 80 μL of protein A/G beads (0.5 mL agarose in 2.0 mL PBS buffer with 0.02% azide) (Santa Cruz Biotechnology, Dallas, TX) were then added to the solution for an overnight incubation at 4°C with gentle rotation. The supernatant was removed by carefully washing the beads once with 200 μL of binding buffer once, 200 μL of washing buffer 1 (50 mM Tris HCl [pH 8.0], 100 mM NaCl, 1 mM EDTA) twice, 200 μL of washing buffer 2 (50 mM Tris [pH 8.0], 100 mM NaCl, 1 mM EDTA, 10% acetonitrile [ACN]) once, and 200 μL of water once. The nitrotyrosine-containing peptides were eluted with 20 μL of 0.5% TFA/25% ACN. The elution step was repeated twice and the eluates combined and dried with a SpeedVac. The nitrotyrosine-containing peptides were resuspended in 0.1% TFA and desalted with C18 ZipTips (EMDMillipore, Billerica, MA) before MS analysis.

Nano LC-MS/MS Analysis

The desalted peptides were reconstituted in 20 μL 4% ACN/0.1% formic acid. All peptide samples were separated on an online nanoflow Easy nLC1000 UHPLC system (Thermo Scientific, San Jose, CA) and analyzed on a Q Exactive Orbitrap mass spectrometer (Thermo Scientific). Ten μL of sample was injected onto a capillary peptide trap column (Acclaim® Pepmap 100, 75 μm × 2 cm, C18, 3 μm, 100 Å, Thermo Scientific). After sample injection, the peptides were separated on a 25-cm UHPLC reversed-phase column (Acclaim® Pepmap 100, 75 μm × 25 cm, C18, 2 μm, 100 Å, Thermo Scientific) at a flow rate of 300 nL/min. A 4-h linear gradient from 2% solvent A (0.1% formic acid in water) to 35% solvent B (0.1% formic acid in ACN) was used for each LC-MS/MS run. Data-dependent acquisition was performed using Xcalibur 2.2 software in positive ion mode at a spray voltage of 2.1 kV. Survey spectra were acquired in the Orbitrap with a resolution of 70,000, a maximum injection time of 80 ms, an automatic gain control (AGC) of 1e6, and a mass range from 400 to 1400 *m/z*. The top 10 ions in each survey scan were selected for higher-energy collisional dissociation scans with a resolution of 17,500. For all higher-energy collisional dissociation scans, collision energy was set to 30, the maximum inject time was 60 ms, and the AGC was 1e5. The isolation window for precursors is 4 Da. The intensity threshold for triggering MS2 is 1.7E4. The ions with 2+ and 3+ charges were selected for MS2. Ions selected for MS/MS were dynamically excluded for 30 s after fragmentation.

Mass spectrometry data analysis

All mass spectra were processed using Proteome Discoverer v1.4 (Thermo Scientific, San Jose, CA) with SEQUEST algorithm.[38] The databases used for proteins peptide identifications were SwissProt bovine protein sequence database (5975 protein entries, downloaded at Feburary 21, 2013), SwissProt human protein sequence database (20,247 protein entries, downloaded at Feburary 21, 2013) or SwissProt mouse sequence database (containing 16,900 mouse protein entries, download at December 26, 2015). The parameters for database search were full trypsin digestion; a mass tolerance of ± 10 ppm for precursor

Author Manuscript Author Manuscript Author Manuscript Author Manuscript

and product ions with a maximum of two missed cleavage sites permitted; static mass modifications included carbamidometheylation on cysteinyl residues. Variable modifications were oxidation of methionine and nitration of tyrosine residues (+44.9851 Da). The FDR (false discovery rate) cutoff for peptide and protein identification was 0.01 based on targeted-decoy-based approach. The detail parameters for SEQUEST database search were listed in Supplemental table S1.

The normalized spectral abundance factor (NSAF) value for each protein was calculated as described in Equation 1,[39]

$$(\mathrm{NSAF})_k=(I/L)_k/\sum_{i=1}^{N}(I/L)_i \quad \text{(Eq. 1)}$$

where the total MS intensity (I) of the matching peptides from protein k is divided by the protein length (L), and then divided by the sum of I/L for all uniquely identified proteins in the dataset.

Label-free quantification of nitrotyrosine peptides in mouse lung

Mass spectra were analyzed using MaxQuant software version 1.5.2.8 using the Andromeda search engine.[40,41] The initial maximum allowed mass deviation was set to 20 ppm for monoisotopic precursor ions and MS/MS peaks. The mass tolerance for main peptide search was set at 4.5 ppm. Enzyme specificity was set to trypsin, defined as N-terminal to arginine and lysine excluding proline, and allowing a maximum of two missed cleavages. Carbamidomethylcysteine was set as a fixed modification, and N-terminal acetylation, methionine oxidation, and nitration of tyrosine as variable modifications. The spectra were searched by the Andromeda search engine against the mouse SwissProt sequence database (containing 16,900 mouse protein entries, download at December 26, 2015) combined with 248 common contaminants and concatenated with the reversed versions of all sequences. Quantification in MaxQuant was performed using the built in XIC-based label-free quantification (LFQ) algorithm.[40] The required false positive rate for identification was set to 1% at the peptide and 1% at the protein level, and the minimum required peptide length was set to six amino acids. Contaminants, reverse peptide identification were excluded from further data analysis. The detail parameters for MaxQuant database search were listed in Supplemental table S1. The LFQ values were log2-transfomed. After filtering (at least 6 valid LFQ values in at least one group), remaining missing LFQ values were imputed from a normal distribution (width, 0.3; down shift, 1.8). For statistical analysis of MaxQuant output we used the Perseus platform (Version 1.5.5.3).[42] A two- sample Student's *t*-test was used to assess statistical significance of the abundance of nitrotyrosine peptides using Permutation-based FDR below 0.01 as the cutoff.

The mass spectrometry proteomics data have been deposited to the ProteomeXchange Consortium [43] via the PRIDE partner repository with the dataset identifiers PXD005320 and PXD006427.

Author Manuscript Author Manuscript Author Manuscript Author Manuscript

RESULTS AND DISCUSSION

Antibody-based enrichment strategy for nitrotyrosine peptides

Our antibody-based enrichment strategy (Supplemental Fig. S1) involves protein digestion and specific immunoprecipitation (IP) of the NT-containing peptides with an anti-NT mAb (clone 39B6). The antibody-NT peptide complexes are captured by protein A/G beads, separated from non-nitrated peptides, and washed. Finally, the captured NT-containing peptides are eluted from the beads with a low-pH solution. The clone 39B6 Ab is a mouse mAb to 3-Nitrotyrosine that was raised against a 3-(4-Hydroxy-3-nitrophenyl acetamido) propionic acid-BSA conjugate. The reasons why we chose this mAb are two-fold. First, use of a monoclonal mAb enables standardization of the approach and can avoid the lot-lot variability typically seen with polyclonal Ab preparations. Second, in a previously reported molecular recognition specificity study of anti-3-nitrotyrosine Abs, the binding affinities of the clone 39B6 mAb showed significant binding activity for all six synthetic nitrotyrosine peptides tested, in contrast to other anti-nitrotyrosine Abs whose recognition specificity was dependent on the sequence motif flanking the modified tyrosine.[34,35] This is probably because this mAb was raised against a 3-(2-(4-hydroxy-3-nitrophenyl) acetamido) propionyl-bovine serum albumin conjugate in which the (4-hydroxy)-3-nitrophenyl group is more exposed and freely accessible compared to the NT residues in the polypeptide chains of nitrated carrier proteins used as antigens for the production of Abs.

Efficiency of IP enrichment for nitrotyrosine peptides

To test the specificity of the clone 39B6 mAb and the feasibility of this immunoaffinity method, we used it to enrich the NT-containing peptides from tryptic digest of nitrated BSA. With IP enrichment, we identified 18 and 17 nitrotyrosine peptides from two replicates, respectively (Fig. 1A). A total 19 BSA nitrotyosine peptides with various site locations and flanking sequences were identified. (Table 1, annotated MS/MS spectra of nitrotyosine peptides shown in Supplemental data S1, and SEQEUST database searching results were listed in Supplemental table S2). These data confirmed that the clone 39B6 anti-NT mAb has high affinity for binding NT peptides independent of the position of the NT sites within the peptides and the sequence motif of the peptides.

Next, we evaluated the efficiency of the IP enrichment for NT-containing peptides. Due to the nature of data-dependent data acquisition of mass spectrometry, the value of peptide spectrum matches (PSMs) is positively correlated with the relative abundance of the peptides in the sample, where a highly abundant peptide would be selected for MS/MS more frequently, and so has a higher PSM value. We compared the number of PSMs of NT peptides and non-nitrated peptides of BSA before (input) and after IP enrichment. LC-MS analysis identified 1,437 and 479 BSA PSMs from the input and IP samples, respectively (Supplemental table S2). In the input sample, the majority of PSMs (1,340, 93% of total BSA PSMs) are to non-nitrated BSA peptides, and only 97 (7%) of the PSMs are to NT-containing peptides (Fig. 1B), indicating that NT-containing peptides are much less abundant than the non-nitrated peptides in the BSA tryptic digest. With IP enrichment, we eliminated the majority of non-nitrated peptides. Many non-nitrated BSA peptides with a large number of PSMs that were identified in the input BSA tryptic digest were not detectable in the anti-

Author Manuscript Author Manuscript Author Manuscript Author Manuscript

NT IP sample (Supplemental table S3), suggesting that IP enrichment effectively removed non-nitrated peptide contamination. By contrast, NT-containing peptides were significantly enriched by IP. The enrichment greatly increased the detectability of NT-containing peptides by MS, and the number of PSMs of NT-containing peptides (Table 1). As shown in Fig 1B, of 479 PSMs of BSA peptides after IP, 434 (91%) were NT-containing peptides, and only 45 (9%) were non-nitrated peptides, indicating an enrichment factor of about 10-fold. As a consequence, we identified six more NT sites and three peptides with multiple NT sites that were not detectable in the analysis of the input sample.

IP enrichment for nitrotyrosine peptides from a whole-cell lysate

We next applied this strategy to a more complex system – the whole-cell lysate from A549 human alveolar adenocarcinoma cells. The whole-cell lysate was first nitrated *in vitro*, the proteins digested, and the peptides subjected to MS analysis before and after anti-nitrotyrosine antibody enrichment. LC-MS/MS analysis of the tryptic peptides of the whole-cell lysate (input) identified 17,118 (95% of total identified unique peptides) non-nitrated peptides and 965 (5% of total identified unique peptides) NT-containing peptides. Of 71,503 PSMs, 95% (67,835) were to non-nitrated peptides and 5% (3,668) were to NT-containing peptides (Supplemental table S4). After IP- enriched fraction, we identified 1,354 and 1,287 nitrotyrosine peptides from two technical replicates, respectively (Supplemental table S5). The overlap of the identified NT-containing peptides between the two replicates is high (80%) and the correlation of the intensity of the peptide is very good (r = 0.88), indicating that this method has excellent reproducibility (Supplemental Fig. S2A, B). By combining the two replicates, we identified 1,559 (43% of total identified peptides) unique NT-containing peptides including 248 peptides with two nitrotyrosine sites, 28 peptides with three nitrotyrosine sites, and six peptides with four nitrotyrosine sites. High-resolution Orbitrap mass spectrometry enables identification of nitrotyrosine site with high confidence, even for peptides with more than one nitrotyrosine site. Two representative product ion spectra are shown in Fig. 2A and B for two nitrotryosine-containing peptides [Y(NO_2)LNTNPVGGLLEY(NO_2)AR from double-stranded RNA-specific adenosine deaminase (ADAR); DGY(NO_2)DY(NO_2)DGY(NO_2)R from serine/arginine-rich splicing factor 1 (SRSF1)]. Each of these two peptides has more than one nitrotyrosine site. The product ion spectrum quality is high enough for unambiguous identification of the peptide sequence and the nitrotyrosine sites as well. The annotated MS/MS spectra of all identified nitrotyosine peptides are shown in Supplemental data S1.

Treatment of proteins with peroxynitrite can result in additional modfications besides of tyrosine nitration, such as tryptophan nitration, lysine formylation, and cysteine oxidation.[44] We identified 51 peptides with tryptophan nitration, 164 peptides with lysine formylation, and 224 peptides with cysteine oxidation. From the IP enriched fraction, we identified 39 peptides with tryptophan nitration , 40 peptides with lysine formylation and 17 cysteine oxidation (Supplemental table S4 and S5).

IP enrichment significantly increases the detectability of NT-containing peptides. As shown in Fig 3A, the percentage of NT peptides was increased from 5% to 43% after IP enrichment. The proportion of NT-containing peptides to all identified peptides is higher

Author Manuscript Author Manuscript Author Manuscript Author Manuscript

than the enrichment of acetylated lysine peptides with an anti-acetyl-lysine Ab.[45] Our IP enrichment eliminates about 87% of the PSMs of non-nitrated peptides (Supplemental Fig. 2C). Inspection of the abundance rank plots of the most abundant non-nitrated peptides (PSMs>1) in the input sample vs the IP-enriched fraction show that the relative amount of non-nitrated peptides in IP sample was greatly reduced (Fig. 3B). The identified non-nitrated peptides carried along during the IP enrichment process are from the most abundant proteins such as Keratin 8 (KRT8), Actin (ACTC1) and Annexin A2 (ANXA2). The detection of these high-abundance peptides is likely due to non-specific binding of these peptides to the protein A/G beads. The washing after mAb capture was able to greatly reduce the amount of these non-nitrated peptides on the beads, but because of the high sensitivity of mass spectrometry, even trace amounts of non-nitrated peptides remaining in the IP fraction can be detected.

This immuno-affinity enrichment not only increases the number of identified NT peptides, but also the number of identified NT-containing proteins. The number of NT-containing proteins identified after IP enrichment was more than twice the number of NT-containing proteins identified in the input (Fig. 3C).

We further evaluated whether this strategy can increase the detectability of low-abundance NT-containing proteins. We used the normalized spectral abundance factor (NSAF) to compare the relative abundances of the NT-containing proteins in the input and the anti-NT IP-enriched fraction. The NSAF is based on spectral counting, which has been widely used in label-free proteomics quantitation. In spectral counting, larger proteins usually generate more peptides, and therefore more spectral counts, than smaller proteins. Therefore, the number of spectral counts for each protein is first divided by the mass or protein length, which defines the spectral abundance factor (SAF). Furthermore, to accurately account for sample to sample variation, individual SAF values are normalized to one by dividing them by the sum of all SAFs for proteins identified in the sample, resulting in the NSAF value.[39] In this way NSAF values are standardized across distinct samples, allowing direct comparisons between individual samples. The NSAF value of one protein is positively correlated with the relative abundance of the protein in the sample, and a highly abundant protein will have a higher NSAF value. We calculated the NSAF value for each protein identified in the IP-enriched fraction and input, and then compared their NSAF scores in the IP-enriched fraction and input. As shown in Fig. 3D, the histogram of the NT-containing proteins in the IP-enriched fraction was shifted to the left compared with that of the input, indicating that more low-abundance NT-containing proteins were identified via our IP enrichment strategy.

This immunoaffinity enrichment approach identified 1,559 NT peptides (with 1,881 NT sites), far more than did chemical derivatization methods such as SPEAR (Solid-Phase Active Easter Reagent)[29] and ANSID (Aromatic Nitration Site Identification) methods[28]. SPEAR identified 34 NT peptides from *in vitro* nitrated plasma,[29] and ANSID identified 244 nitrotyrosine peptides from *in vitro* nitrated rat brain.[28] The advantages of immunoaffinity enrichment over current chemical derivatization methods are several. First, it does not require multi-step chemical reactions, which avoids the low yield of chemical reactions and the sample losses common during multiple-step sample processing. Secondly,

Author Manuscript Author Manuscript Author Manuscript Author Manuscript

our approach does not require introducing any affinity tags, and therefore eliminates concerns about chemical tags or concomitant chemical derivatization (such as tyrosine sulfation) changing the MS/MS fragmentation pattern and interfering with protein database searching.[30,31] Finally, our approach uses routine IP, a technique widely practiced in research laboratories, and is much simpler than chemical derivatization methods.

Cross-reactivity of the anti-nitrotyrosine antibody

Peroxynitrite can react with other amino acids such as cysteine and tryptophan, leading to oxidation of cysteine and nitration of tryptophan.[46] The specificity of our antibody against nitrotyrosine peptides is a key factor for the success of our approach. Serval previous publications state that immunoprecipitation of nitrotyrosine-containing peptides is less feasible for proteomic analysis of NT-containing proteins in a complex proteome due to cross-reactivity to other nitrated amino acids and low affinity of the antibody.[17,29] For instance, it was reported that one commercially available antibody directed against 3-Nitrotyrosine (clone 1A6) has cross-reactivity for the tryptophan derivative 5-hydroxy-6-nitrotryptophan due to the structural similarities between 3-nitrotyrosine and 5-hydroxy-6-nitrotryptophan.[23] We were unable to find any reports in the literature on the cross-reactivity of the clone 39B6 mAb with 5-hydroxy-6-nitrotryptophan. To address this question experimentally, we performed protein database searching with various nitrations of the tryptophan residue. From LC-MS/MS analysis of the *in vitro* nitrated A549 cell extract, 51 peptides containing 5-hydroxy-6-nitrotryptophan were identified. After IP enrichment with the 39B6 antibody, the number of identified peptides containing 5-hydroxy-6-nitrotryptophan decreased to 39, indicating that the 3-nitrotyrosine-directed clone 39B6 mAb used in our study does not enrich peptides containing 5-hydroxy-6-nitrotryptophan.

Reproducibility of IP enrichment for nitrotyrosine peptides—We used *in vitro* nitrated mouse lung to evaluate the reproducibility of the method. *In vitro* nitration was performed with the same procedure used in *in vitro* nitrated whole cell lysate. Five technical replicates of IP enrichment were performed. LC-MS/MS analysis identified 779, 677, 685, 534, and 736 nitrotyrosine peptides, respectively (Supplemental Table S6). There was significant overlap of nitrated peptides identified from five replicates. A total of 436 (>50%) nitrotyrosine peptides were identified from all of the five replicates (Fig. 4A). We further used label free approach to evaluate the quantitative reproducibility. We plotted the intensities of the nitrotyrosine peptides between the replicates. As shown in the multiple scatter plots (Fig. 4B), the intensities of the peptide showed excellent correlation between the replicates. The Pearson correlation was between 0.78 −0.94. We also evaluate the reproducibility of enrichment efficiency. The proportion of NT-containing peptides to all identified peptides was about 50% and was very consistent across the replicates (Fig. 4C).

Antibody specificity for the location of nitrotyrosine within the peptides—We have demonstrated that antibody 39B6 has high specificity for nitrotyrosine peptides relative to non-nitrated peptides and did not cross-react with other nitrated amino acids. We further evaluate the affinity of the antibody to the location of nitrotyrosine site. In the nitrated cell lysate and mouse lung study, we identified many nitrotyrosine peptides with various site locations, but we noticed that a large proportion of identified nitrotyrosine peptides had the

Author Manuscript Author Manuscript Author Manuscript Author Manuscript

modification site on position one (N-terminal tyrosine). For example, in nitrated cell lysate study, out of 1,881 identified nitrotyrosine sites, 1,310 (69.6%) had the nitrotyrosine site at position one; and out of 1,192 identified nitrotyrosine sites identified in nitrated mouse lung, 490 (41.1%) had the nitrotyrosine site at position one. We did the sequence logo analysis of identified nitrotyrosine peptides from these two studies. As shown in Fig. 4D, the peptides with sequence K/RY were enriched in these two datasets. We further investigate whether the antibody had site location bias. To test that, we digested the nitrated cell lysate of A549 cells with a different enzyme, Endoproteinase Glu-C, which selectively cleaves peptide bonds N-terminal to glutamic acid residues. In this study, we identified less number of peptides from input sample and also the IP enrichment fraction probably due to less efficiency of Glu-C digestion relative to trypsine (Supplemental table S7). LC-MS/MS analysis of IP enrichment fraction showed that out of 98 identified nitrotyrosine sites, 68 (69.3%) had the nitrotyrosine site at position one. The sequence logo analysis of this dataset was shown in Fig. 4D. Taken together, the data suggested that 39B6 mAb had stronger affinity for the peptides with N-terminal nitortyrosine. It may be because the 39B6 mAb was raised against a 3-(2-(4-hydroxy-3-nitrophenyl) acetamido) propionyl-bovine serum albumin conjugate, and it was shown to have higher affinity to single 3-nitrotyrosine amino acid compared to nitrotyrosine residue in the polypeptide chain of nitrated carrier protein used as antigen for the production of antibodies [35]. The structure of peptides with N-terminal nitrotyrosine was similar to the epitope of 39B6 mAb, and the (4-hydroxy)-3-nitrophenyl group at the N-terminal tyrosine is more exposed and freely accessible. These are probably the factors that contribute to higher affinity of 39B6 mAb to peptides with N-terminal nitrotyrosine. This study provided a proof of concept for using immunoaffinity method to enrich nitrotyrosine peptides for proteomics analysis. Ideally, the affinity of the antibody for this enrichment method should have high affinity for binding nitrotyrosine peptides independent of position of the nitrotyrosine sites within the peptides and the sequence motif of the peptides. Our data indicate that 39B6 mAb has good affinity and specificity for nitrotyrosine peptides, and from the sequence log analysis, we also found no evidence to indicate that the affinity of antibody is dependent on the sequence motif flanking the modified tyrosine. However, the antibody does show higher affinity to peptides with N-terminal nitrotyrosine. In future study, developing a pan-specific nitrotyrosine antibody can ensure an unbiased, proteome-wide analysis of tyrosine nitration.

Quantitative profiling for protein nitrotyrosine

To assess whether our approach for enriching nitrotyrosine peptides can be used for quantitative analysis of protein tyrosine nitration in a complex biological sample, we combined this immunoaffinity method with label-free quantification to analyze the changes in protein nitrotyrosine in the mouse lung after inducing inflammation via dsRNA [poly(I:C)] treatment. Extracellular poly(I:C) is a viral molecular pattern that potently triggers a protective inflammatory response involving the production of soluble type I and –III interferons (IFNs);[47–49] C-, CXC- and CC-type chemokines;[50–52] and nitric oxide synthase.[53–55] Poly(I:C) is thus a validated model for studying dynamic changes in protein tyrosine nitration. Using our immunoaffinity enrichment approach, we identified 862 unmodified peptides and 248 nitrotyrosine peptides. Out of 248 nitrotyrosine peptides, 147 nitrotyrosine peptides containing 237 nitrotryrosine sites were quantified (Supplemental table S8). The annotated MS/MS spectra of all identified NT peptides are shown in

Author Manuscript Author Manuscript Author Manuscript Author Manuscript

Supplemental data1. The animal-to-animal Pearson correlation of peptide quantification within each experimental group ranged from 0.41–0.82, indicating good reproducibility of quantification within each experimental group (Figure 5A, Supplemental Fig. S3). A two-sample Student's *t*-test identified 86 NT sites that were significantly changed upon poly(I:C) treatment (presumption-based FDR 0.01) (Figure 5B). Among them, 14 NT peptides, including Tyr69 of superoxide dismutase [Mn] (SOD2) and Tyr445 of protein-glutamine gamma-glutamyltransferase 2 (TGF2) were upregulated upon poly(I:C) treatment; and 72 NT sites were downregulated (Supplemental table S8). According to the PhosphoSitePlus database (www.phosphosite.org),[56] of 135 significantly changed NT sites, 35 are known to potentially be phosphorylated. It is not clear whether the nitration affects phosphorylation on these sites.

Virus-induced airway inflammation causes epithelial damage and repair, a major pathophysiological process mediating chronic lung diseases.[57] Our data clearly show that poly(I:C) induces changes in protein tyrosine nitration in the mouse lung. Although the functions of these tyrosine nitration events are still unknown, the data can be used for future hypothesis-driven studies on the roles of these tyrosine nitration events in regulating airway injury and repair.

CONCLUSIONS

Protein nitration has emerged as an interesting posttranslational protein modification due to its prominent roles in diseases related to nitro/oxidative stress. We describe a simple, reproducible new nitrotyrosine peptide enrichment strategy that captures the nitrotyrosine peptides with an mAb with high affinity for NT peptides independent of the site of NT modification and the peptide sequence motif. The feasibility and efficiency of this method was demonstrated by identifying 1,861 NT sites in an *in vitro* nitrated whole-cell lysate. To our knowledge, this method produces the largest coverage of nitrotyrosine sites from a complex proteome sample. We have demonstrated that this method can also be used for a quantitative analysis of protein tyrosine nitration by coupling with a label-free approach, which can be very useful for profiling changes in tyrosine nitration under different biological conditions. Our study demonstrated that the antibody used in this study had higher affinity to peptide with C-terminal nitrotyrosine relative to peptides with other nitrotyrosine locations, which raises the need for future study to develop a pan-specific nitrotyrosine antibody for unbiased, proteome-wide analysis of tyrosine nitration.

Supplementary Material

Refer to Web version on PubMed Central for supplementary material.

Acknowledgments

This work was supported by National Institutes of Health Grants NCATS UL1TR001439 (to ARB), DMS-1361411/DMS-1361318 (ARB, YZ), NIAID AI062885 (ARB), NIEHS P30 ES006676 (ARB) and pilot funding from the Sealy Center for Molecular Sciences (SCMM-SysBio-2016). We thank Dr. David Konkel for critically editing the manuscript.

Author Manuscript Author Manuscript Author Manuscript Author Manuscript

Abbreviations

AGC	automatic gain control
BSA	bovine serum albumin
DTT	dithiothreitol
FDR	false discovery rate
IP	immunoprecipitation
LC	liquid chromatography
mAb	monoclonal antibody
MS	mass spectrometry
NSAF	normalized spectral abundance factor
PSM	peptide spectrum match
RNS	reactive nitrogen species
SAF	spectral abundance factor
UHPLC	ultra-high performance liquid chromatography

References

1. Sugiura H, Komaki Y, Koarai A, Ichinose M. Nitrative stress in refractory asthma. J Allergy Clin Immunol. 2008; 121:355–60. [PubMed: 18158173]
2. Voraphani N, Gladwin MT, Contreras AU, Kaminski N, Tedrow JR, Milosevic J, Bleecker ER, Meyers DA, Ray A, Ray P, Erzurum SC, Busse WW, Zhao J, Trudeau JB, Wenzel SE. An airway epithelial iNOS-DUOX2-thyroid peroxidase metabolome drives Th1/Th2 nitrative stress in human severe asthma. Mucosal Immunol. 2014; 7:1175–85. [PubMed: 24518246]
3. Cobb CA, Cole MP. Oxidative and nitrative stress in neurodegeneration. Neurobiol Dis. 2015; 84:4–21. [PubMed: 26024962]
4. Schildknecht S, Gerding HR, Karreman C, Drescher M, Lashuel HA, Outeiro TF, Di Monte DA, Leist M. Oxidative and nitrative alpha-synuclein modifications and proteostatic stress: implications for disease mechanisms and interventions in synucleinopathies. J Neurochem. 2013; 125:491–511. [PubMed: 23452040]
5. Parastatidis I, Thomson L, Fries DM, Moore RE, Tohyama J, Fu X, Hazen SL, Heijnen HF, Dennehy MK, Liebler DC, Rader DJ, Ischiropoulos H. Increased protein nitration burden in the atherosclerotic lesions and plasma of apolipoprotein A-I deficient mice. Circ Res. 2007; 101:368–76. [PubMed: 17615369]
6. Thomson L, Tenopoulou M, Lightfoot R, Tsika E, Parastatidis I, Martinez M, Greco TM, Doulias PT, Wu Y, Tang WH, Hazen SL, Ischiropoulos H. Immunoglobulins against tyrosine-nitrated epitopes in coronary artery disease. Circulation. 2012; 126:2392–401. [PubMed: 23081989]
7. Jayakumari NR, Reghuvaran AC, Rajendran RS, Pillai VV, Karunakaran J, Sreelatha HV, Gopala S. Are nitric oxide-mediated protein modifications of functional significance in diabetic heart? ye'S, -NO', wh'Y-NO't? Nitric Oxide. 2014; 43:35–44. [PubMed: 25153035]
8. Choudhari SK, Chaudhary M, Bagde S, Gadbail AR, Joshi V. Nitric oxide and cancer: a review. World J Surg Oncol. 2013; 11:118. [PubMed: 23718886]

Author Manuscript Author Manuscript Author Manuscript Author Manuscript

9. Yeo WS, Kim YJ, Kabir MH, Kang JW, Ahsan-Ul-Bari M, Kim KP. Mass spectrometric analysis of protein tyrosine nitration in aging and neurodegenerative diseases. Mass Spectrom Rev. 2015; 34:166–83. [PubMed: 24889964]
10. Franco MC, Ricart KC, Gonzalez AS, Dennys CN, Nelson PA, Janes MS, Mehl RA, Landar A, Estevez AG. Nitration of Hsp90 on Tyrosine 33 Regulates Mitochondrial Metabolism. J Biol Chem. 2015; 290:19055–66. [PubMed: 26085096]
11. Aggarwal S, Gross CM, Rafikov R, Kumar S, Fineman JR, Ludewig B, Jonigk D, Black SM. Nitration of tyrosine 247 inhibits protein kinase G-1alpha activity by attenuating cyclic guanosine monophosphate binding. J Biol Chem. 2014; 289:7948–61. [PubMed: 24469460]
12. Corpas FJ, Leterrier M, Begara-Morales JC, Valderrama R, Chaki M, Lopez-Jaramillo J, Luque F, Palma JM, Padilla MN, Sanchez-Calvo B, Mata-Perez C, Barroso JB. Inhibition of peroxisomal hydroxypyruvate reductase (HPR1) by tyrosine nitration. Biochim Biophys Acta. 2013; 1830:4981–9. [PubMed: 23860243]
13. Teng RJ, Wu TJ, Afolayan AJ, Konduri GG. Nitrotyrosine impairs mitochondrial function in fetal lamb pulmonary artery endothelial cells. Am J Physiol Cell Physiol. 2016; 310:C80–8. [PubMed: 26491046]
14. Guo W, Adachi T, Matsui R, Xu S, Jiang B, Zou MH, Kirber M, Lieberthal W, Cohen RA. Quantitative assessment of tyrosine nitration of manganese superoxide dismutase in angiotensin II-infused rat kidney. Am J Physiol Heart Circ Physiol. 2003; 285:H1396–403. [PubMed: 12791589]
15. Monteiro HP, Arai RJ, Travassos LR. Protein tyrosine phosphorylation and protein tyrosine nitration in redox signaling. Antioxid Redox Signal. 2008; 10:843–89. [PubMed: 18220476]
16. Li B, Held JM, Schilling B, Danielson SR, Gibson BW. Confident identification of 3-nitrotyrosine modifications in mass spectral data across multiple mass spectrometry platforms. J Proteomics. 2011; 74:2510–21. [PubMed: 21514405]
17. Zhan X, Wang X, Desiderio DM. Mass spectrometry analysis of nitrotyrosine-containing proteins. Mass Spectrom Rev. 2015; 34:423–48. [PubMed: 24318073]
18. Peng F, Li J, Guo T, Yang H, Li M, Sang S, Li X, Desiderio DM, Zhan X. Nitroproteins in Human Astrocytomas Discovered by Gel Electrophoresis and Tandem Mass Spectrometry. J Am Soc Mass Spectrom. 2015; 26:2062–76. [PubMed: 26450359]
19. Piroddi M, Palmese A, Pilolli F, Amoresano A, Pucci P, Ronco C, Galli F. Plasma nitroproteome of kidney disease patients. Amino Acids. 2011; 40:653–67. [PubMed: 20676907]
20. Takahashi M, Shigeto J, Sakamoto A, Izumi S, Asada K, Morikawa H. Dual selective nitration in Arabidopsis: Almost exclusive nitration of PsbO and PsbP, and highly susceptible nitration of four non-PSII proteins, including peroxiredoxin II E. Electrophoresis. 2015; 36:2569–78. [PubMed: 26177577]
21. Abello N, Kerstjens HA, Postma DS, Bischoff R. Protein tyrosine nitration: selectivity, physicochemical and biological consequences, denitration, and proteomics methods for the identification of tyrosine-nitrated proteins. J Proteome Res. 2009; 8:3222–38. [PubMed: 19415921]
22. Kanski J, Schoneich C. Protein nitration in biological aging: proteomic and tandem mass spectrometric characterization of nitrated sites. Methods Enzymol. 2005; 396:160–71. [PubMed: 16291231]
23. Nuriel T, Hansler A, Gross SS. Protein nitrotryptophan: formation, significance and identification. J Proteomics. 2011; 74:2300–12. [PubMed: 21679780]
24. Aslan M, Ryan TM, Townes TM, Coward L, Kirk MC, Barnes S, Alexander CB, Rosenfeld SS, Freeman BA. Nitric oxide-dependent generation of reactive species in sickle cell disease. Actin tyrosine induces defective cytoskeletal polymerization. J Biol Chem. 2003; 278:4194–204. [PubMed: 12401783]
25. Brennan ML, Wu W, Fu X, Shen Z, Song W, Frost H, Vadseth C, Narine L, Lenkiewicz E, Borchers MT, Lusis AJ, Lee JJ, Lee NA, Abu-Soud HM, Ischiropoulos H, Hazen SL. A tale of two controversies: defining both the role of peroxidases in nitrotyrosine formation in vivo using eosinophil peroxidase and myeloperoxidase-deficient mice, and the nature of peroxidase-generated reactive nitrogen species. J Biol Chem. 2002; 277:17415–27. [PubMed: 11877405]

Author Manuscript Author Manuscript Author Manuscript Author Manuscript

26. Zhang Q, Qian WJ, Knyushko TV, Clauss TR, Purvine SO, Moore RJ, Sacksteder CA, Chin MH, Smith DJ, Camp DG 2nd, Bigelow DJ, Smith RD. A method for selective enrichment and analysis of nitrotyrosine-containing peptides in complex proteome samples. J Proteome Res. 2007; 6:2257–68. [PubMed: 17497906]
27. Dremina ES, Li X, Galeva NA, Sharov VS, Stobaugh JF, Schoneich C. A methodology for simultaneous fluorogenic derivatization and boronate affinity enrichment of 3-nitrotyrosine-containing peptides. Anal Biochem. 2011; 418:184–96. [PubMed: 21855526]
28. Nuriel T, Whitehouse J, Ma Y, Mercer EJ, Brown N, Gross SS. ANSID: A Solid-Phase Proteomic Approach for Identification and Relative Quantification of Aromatic Nitration Sites. Front Chem. 2015; 3:70. [PubMed: 26779476]
29. Prokai-Tatrai K, Guo J, Prokai L. Selective chemoprecipitation and subsequent release of tagged species for the analysis of nitropeptides by liquid chromatography-tandem mass spectrometry. Mol Cell Proteomics. 2011; 10 M110 002923.
30. Ghesquiere B, Colaert N, Helsens K, Dejager L, Vanhaute C, Verleysen K, Kas K, Timmerman E, Goethals M, Libert C, Vandekerckhove J, Gevaert K. In vitro and in vivo protein-bound tyrosine nitration characterized by diagonal chromatography. Mol Cell Proteomics. 2009; 8:2642–52. [PubMed: 19741252]
31. Ghesquiere B, Goethals M, Van Damme J, Staes A, Timmerman E, Vandekerckhove J, Gevaert K. Improved tandem mass spectrometric characterization of 3-nitrotyrosine sites in peptides. Rapid Commun Mass Spectrom. 2006; 20:2885–93. [PubMed: 16941724]
32. Feeney MB, Schoneich C. Proteomic approaches to analyze protein tyrosine nitration. Antioxid Redox Signal. 2013; 19:1247–56. [PubMed: 23157221]
33. Petre BA, Ulrich M, Stumbaum M, Bernevic B, Moise A, Doring G, Przybylski M. When is mass spectrometry combined with affinity approaches essential? A case study of tyrosine nitration in proteins. J Am Soc Mass Spectrom. 2012; 23:1831–40. [PubMed: 22907170]
34. Dr Gusanu M, Petre BA, Przybylski M. Epitope motif of an anti-nitrotyrosine antibody specific for tyrosine-nitrated peptides revealed by a combination of affinity approaches and mass spectrometry. J Pept Sci. 2011; 17:184–91. [PubMed: 21308874]
35. Petre BA, Dragusanu M, Przybylski M. Molecular Recognition Specificity of Anti-3-Nitrotyrosine Antibodies Revealed by Affinity-Mass Spectrometry and Immunoanalytical Methods. Applications of Mass Spectrometry in Life Safety. 2008:55–67.
36. Yang J, Mitra A, Dojer N, Fu S, Rowicka M, Brasier AR. A probabilistic approach to learn chromatin architecture and accurate inference of the NF-kappaB/RelA regulatory network using ChIP-Seq. Nucleic Acids Res. 2013; 41:7240–59. [PubMed: 23771139]
37. Forbus J, Spratt H, Wiktorowicz J, Wu Z, Boldogh I, Denner L, Kurosky A, Brasier RC, Luxon B, Brasier AR. Functional analysis of the nuclear proteome of human A549 alveolar epithelial cells by HPLC-high resolution 2-D gel electrophoresis. Proteomics. 2006; 6:2656–72. [PubMed: 16586437]
38. Eng JK, McCormack AL, Yates JR. An approach to correlate tandem mass spectral data of peptides with amino acid sequences in a protein database. J Am Soc Mass Spectrom. 1994; 5:976–89. [PubMed: 24226387]
39. Zybailov B, Mosley AL, Sardiu ME, Coleman MK, Florens L, Washburn MP. Statistical analysis of membrane proteome expression changes in Saccharomyces cerevisiae. J Proteome Res. 2006; 5:2339–47. [PubMed: 16944946]
40. Cox J, Hein MY, Luber CA, Paron I, Nagaraj N, Mann M. Accurate proteome-wide label-free quantification by delayed normalization and maximal peptide ratio extraction, termed MaxLFQ. Mol Cell Proteomics. 2014; 13:2513–26. [PubMed: 24942700]
41. Cox J, Mann M. MaxQuant enables high peptide identification rates, individualized p.p.b.-range mass accuracies and proteome-wide protein quantification. Nat Biotechnol. 2008; 26:1367–72. [PubMed: 19029910]
42. Tyanova S, Temu T, Sinitcyn P, Carlson A, Hein MY, Geiger T, Mann M, Cox J. The Perseus computational platform for comprehensive analysis of (prote)omics data. Nat Methods. 2016; 13:731–40. [PubMed: 27348712]

Author Manuscript Author Manuscript Author Manuscript Author Manuscript

43. Vizcaino JA, Deutsch EW, Wang R, Csordas A, Reisinger F, Rios D, Dianes JA, Sun Z, Farrah T, Bandeira N, Binz PA, Xenarios I, Eisenacher M, Mayer G, Gatto L, Campos A, Chalkley RJ, Kraus HJ, Albar JP, Martinez-Bartolome S, Apweiler R, Omenn GS, Martens L, Jones AR, Hermjakob H. ProteomeXchange provides globally coordinated proteomics data submission and dissemination. Nat Biotechnol. 2014; 32:223–6. [PubMed: 24727771]
44. Vana L, Kanaan NM, Hakala K, Weintraub ST, Binder LI. Peroxynitrite-induced nitrative and oxidative modifications alter tau filament formation. Biochemistry. 2011; 50:1203–12. [PubMed: 21210655]
45. Choudhary C, Kumar C, Gnad F, Nielsen ML, Rehman M, Walther TC, Olsen JV, Mann M. Lysine acetylation targets protein complexes and co-regulates major cellular functions. Science. 2009; 325:834–40. [PubMed: 19608861]
46. Alvarez B, Radi R. Peroxynitrite reactivity with amino acids and proteins. Amino Acids. 2003; 25:295–311. [PubMed: 14661092]
47. Garofalo R, Mei F, Manganaro M, Espejo R, Ogra PL, Reyes VE. Upregulation of class I major histocompatibility complex (MHC) molecules on respiratory syncytial virus (RSV)-infected airway epithelial cells. American Journal of Respiratory and Critical Care Medicine. 1994; 149:A987.
48. Jamaluddin M, Wang S, Garofalo RP, Elliott T, Casola A, Baron S, Brasier AR. IFN-beta mediates coordinate expression of antigen-processing genes in RSV-infected pulmonary epithelial cells. Am J Physiol Lung Cell Mol Physiol. 2001; 280:L248–57. [PubMed: 11159003]
49. Tian B, Zhao Y, Kalita M, Edeh CB, Paessler S, Casola A, Teng MN, Garofalo RP, Brasier AR. CDK9-dependent transcriptional elongation in the innate interferon-stimulated gene response to respiratory syncytial virus infection in airway epithelial cells. J Virol. 2013; 87:7075–92. [PubMed: 23596302]
50. Zhang Y, Luxon BA, Casola A, Garofalo RP, Jamaluddin M, Brasier AR. Expression of respiratory syncytial virus-induced chemokine gene networks in lower airway epithelial cells revealed by cDNA microarrays. J Virol. 2001; 75:9044–58. [PubMed: 11533168]
51. Bao X, Liu T, Shan Y, Li K, Garofalo RP, Casola A. Human metapneumovirus glycoprotein G inhibits innate immune responses. PLoS Pathog. 2008; 4:e1000077. [PubMed: 18516301]
52. Bao X, Liu T, Spetch L, Kolli D, Garofalo RP, Casola A. Airway epithelial cell response to human metapneumovirus infection. Virology (New York NY). 2007; 368:91–101.
53. Shin TS, Lee BJ, Tae YM, Kim YS, Jeon SG, Gho YS, Choi DC, Kim YK. Role of inducible nitric oxide synthase on the development of virus-associated asthma exacerbation which is dependent on Th1 and Th17 cell responses. Exp Mol Med. 2010; 42:721–30. [PubMed: 20841959]
54. Mori D, Koide N, Tsolmongyn B, Nagata H, Sano T, Nonami T, Yokochi T. Poly I:C enhances production of nitric oxide in response to interferon-gamma via upregulation of interferon regulatory factor 7 in vascular endothelial cells. Microvasc Res. 2015; 98:68–73. [PubMed: 25582076]
55. Ichikawa T, Sugiura H, Koarai A, Minakata Y, Kikuchi T, Morishita Y, Oka A, Kanai K, Kawabata H, Hiramatsu M, Akamatsu K, Hirano T, Nakanishi M, Matsunaga K, Yamamoto N, Ichinose M. TLR3 activation augments matrix metalloproteinase production through reactive nitrogen species generation in human lung fibroblasts. J Immunol. 2014; 192:4977–88. [PubMed: 24760149]
56. Hornbeck PV, Zhang B, Murray B, Kornhauser JM, Latham V, Skrzypek E. PhosphoSitePlus, 2014: mutations, PTMs and recalibrations. Nucleic Acids Res. 2015; 43:D512–20. [PubMed: 25514926]
57. Lambrecht BN, Hammad H. The airway epithelium in asthma. Nat Med. 2012; 18:684–92. [PubMed: 22561832]
58. Heberle H, Meirelles GV, da Silva FR, Telles GP, Minghim R. InteractiVenn: a web-based tool for the analysis of sets through Venn diagrams. BMC Bioinformatics. 2015; 16:169. [PubMed: 25994840]
59. Crooks GE, Hon G, Chandonia JM, Brenner SE. WebLogo: a sequence logo generator. Genome Res. 2004; 14:1188–90. [PubMed: 15173120]

Author Manuscript Author Manuscript Author Manuscript Author Manuscript

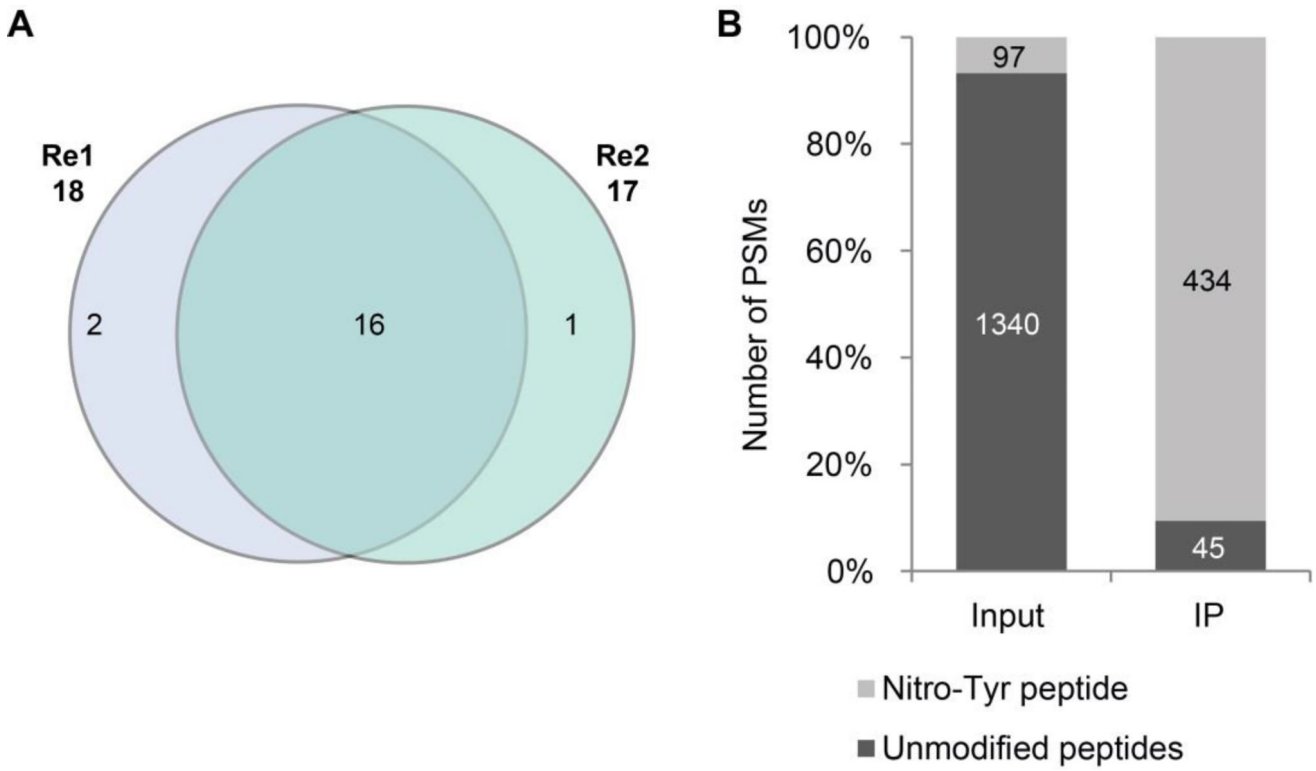

Figure 1.

Feasibility of antibody-based enrichment strategy. The tryptic peptides of *in vitro* nitrated BSA were subjected for anti-tyrosine antibody IP before LC-MS/MS analysis. (A) The overlap of identified nitrotyrosine peptides between replicates. (B) The enrichment of NT-containing peptides by anti-nitrotyrosine antibody. The number on each column are the number of PSM of nitrotyrosine peptides (grey) and non-nitrated peptides (black) identified from each sample. PSM, peptide spectra matched.

Author Manuscript Author Manuscript Author Manuscript Author Manuscript

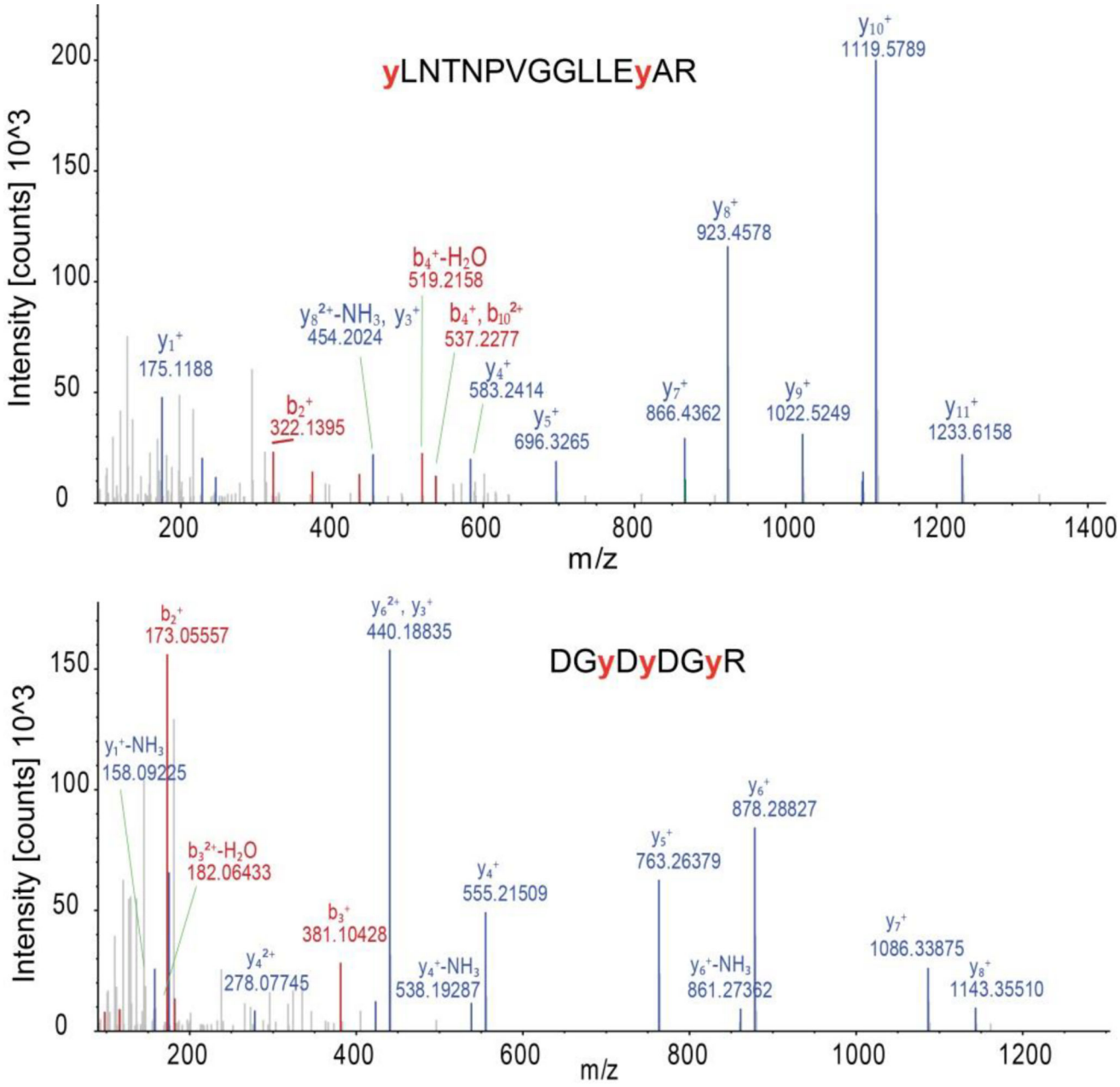

Figure 2.

Annotated MS/MS spectrum of two different nitrotyrosine peptides which were identified from the IP enriched nitrotyrosine peptides mixture of *in vitro* nitrated whole cell lysate of A549 cells. (A) MS/MS spectrum of nitrotyrosine peptide $Y(NO_2)LNTNPVGGLLEY(NO_2)AR$ of protein double-stranded RNA-specific adenosine deaminase (ADAR). (B) MS/MS spectrum of $DGY(NO_2)DY(NO_2)DGY(NO_2)R$ of serine/arginine-rich splicing factor 1 (SRSF1). The red, low case "y" are the tyrosine residues that were nitrated.

Author Manuscript Author Manuscript Author Manuscript Author Manuscript

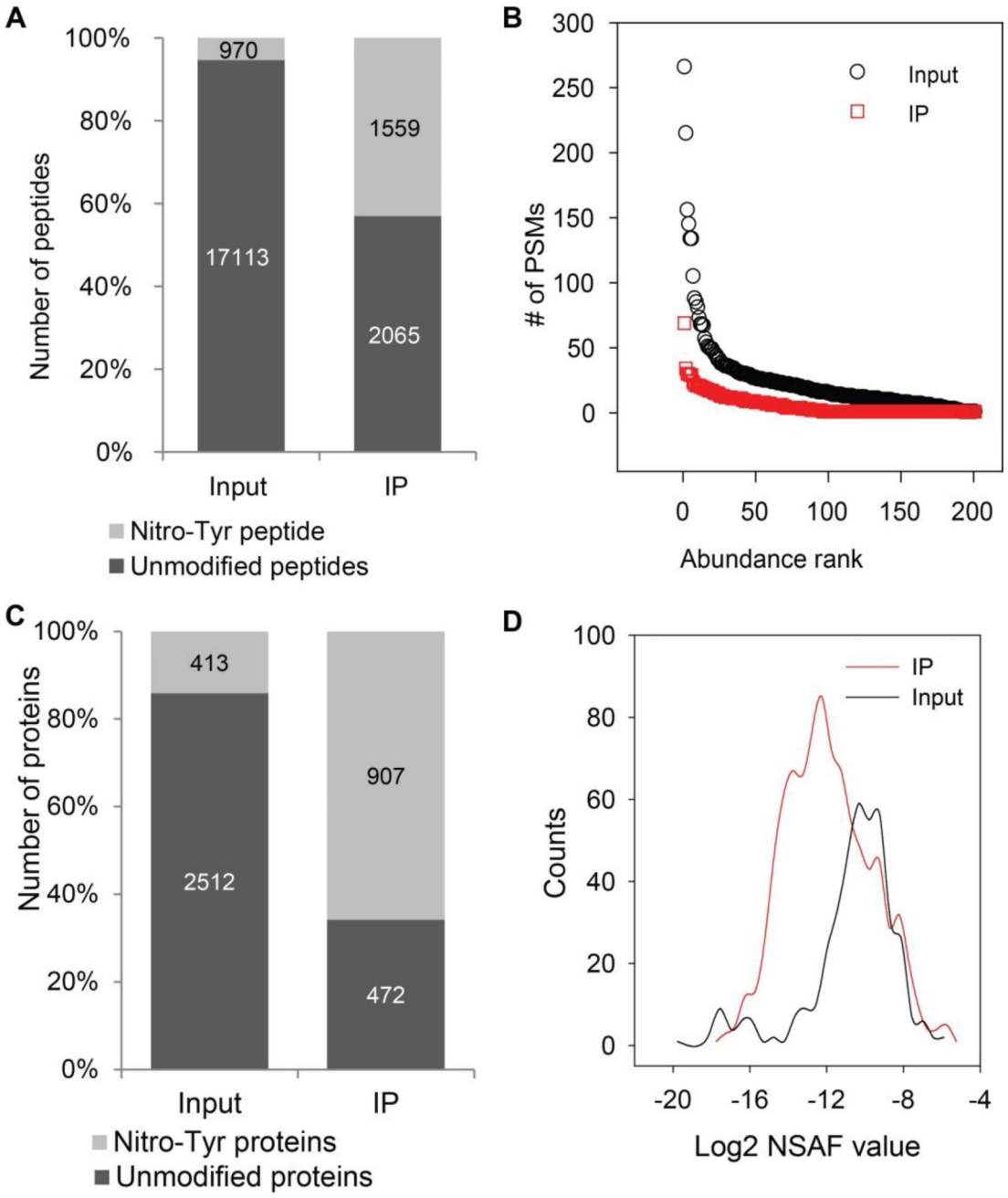

Figure 3.

Enrichment of nitrotyrosine peptides from whole cell lysate of A549 cells. The cell extract was first *in vitro* nitrated, the proteins were digested and the peptides were subjected for MS analysis before and after anti-nitrotyrosine antibody enrichment. (A) The number of non-nitrated peptides (black) and NT-containing peptides (grey) identified from input and IP enriched fraction. (B) The abundance of the non-nitrated peptides relative to all other identified non-nitrated peptides. Black circles, non-nitrated peptides identified from input; red circles, non-nitrated peptides identified from IP fraction. (C) The number of NT-containing proteins (grey) and non-nitrated proteins (black) identified from input and IP

enriched fraction. (D) Histograms of normalized spectra abundance factor (NSAF) for NT-containing proteins identified from input and IP enriched fraction.

Author Manuscript Author Manuscript Author Manuscript Author Manuscript

Author Manuscript Author Manuscript Author Manuscript Author Manuscript

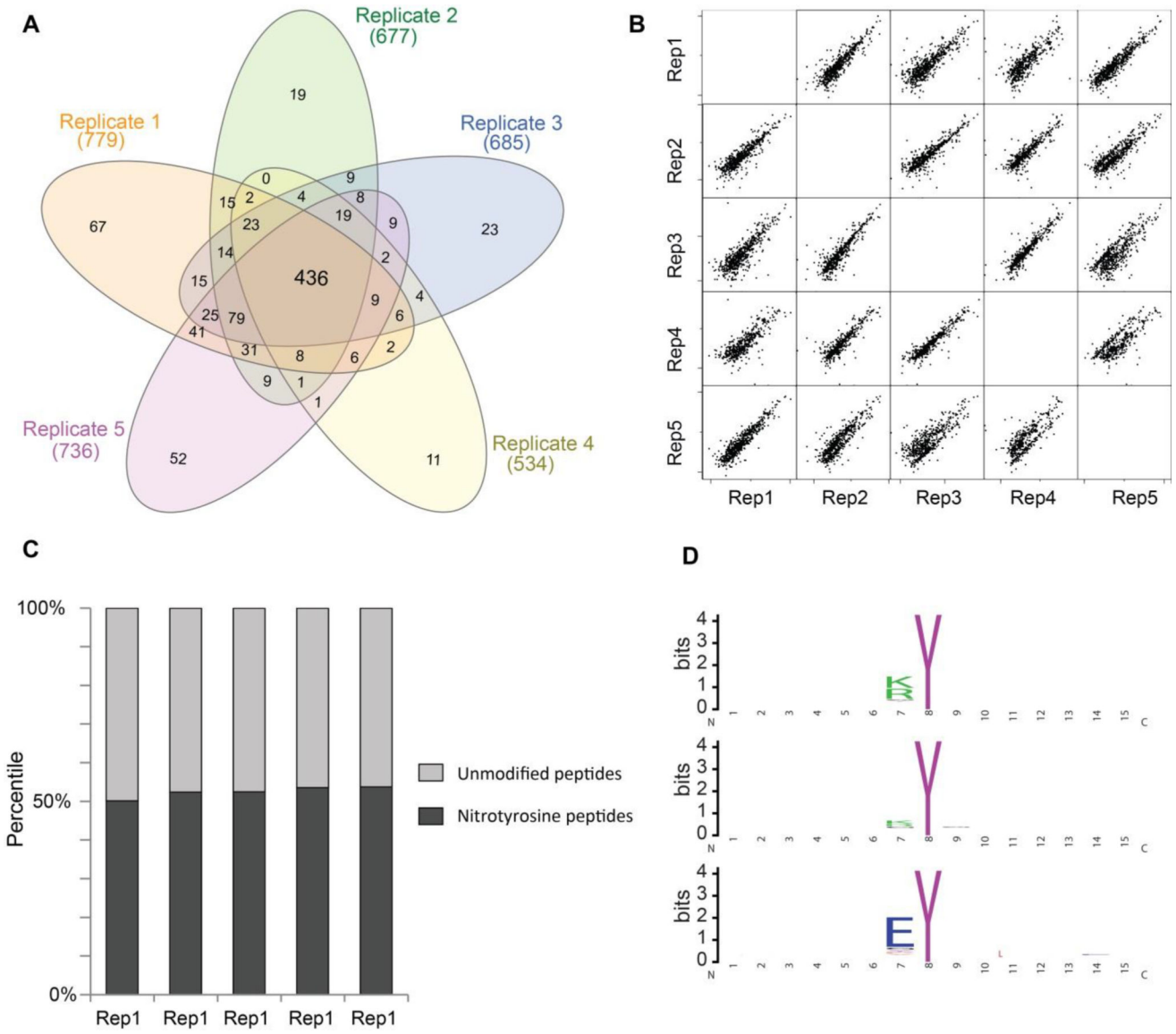

Figure 4.

The reproducibility and site specificity of antibody-based enrichment strategy. The protein extract from one mouse lung was first *in vitro* nitrated and digested with trypsin. The nitrotyrosine peptides were enriched with nitrotyrosine antibody. Five replicates were performed. The IP enriched fractions were subjected for MS analysis. (A) Venn diagram of the overlap of identified NT-containing peptides from five replicates. The Venn diagram was created using InteractiVenn program.[58] (B) Multiple scatter plots of the correlation of the abundance of NT-containing peptides between replicates. (C) Enrichment efficiency of nitrotyrosine peptides from each replicates. (D) Site specificity of antibody-based enrichment strategy. Upper, the sequence logo of all nitrotyrosine peptides identified from nitrated cell lysate that was digested with trypsine; middle, the sequence logo of all nitrotyrosine peptides identified from nitrated mouse lung extract that was digested with trypsine; lower, the sequence logo of all nitrotyrosine peptides identified from nitrated cell

Author Manuscript Author Manuscript Author Manuscript Author Manuscript

lysate which was digested with Glu-C. The sequence logos were generated using Weblogo.[59]

Author Manuscript Author Manuscript Author Manuscript Author Manuscript

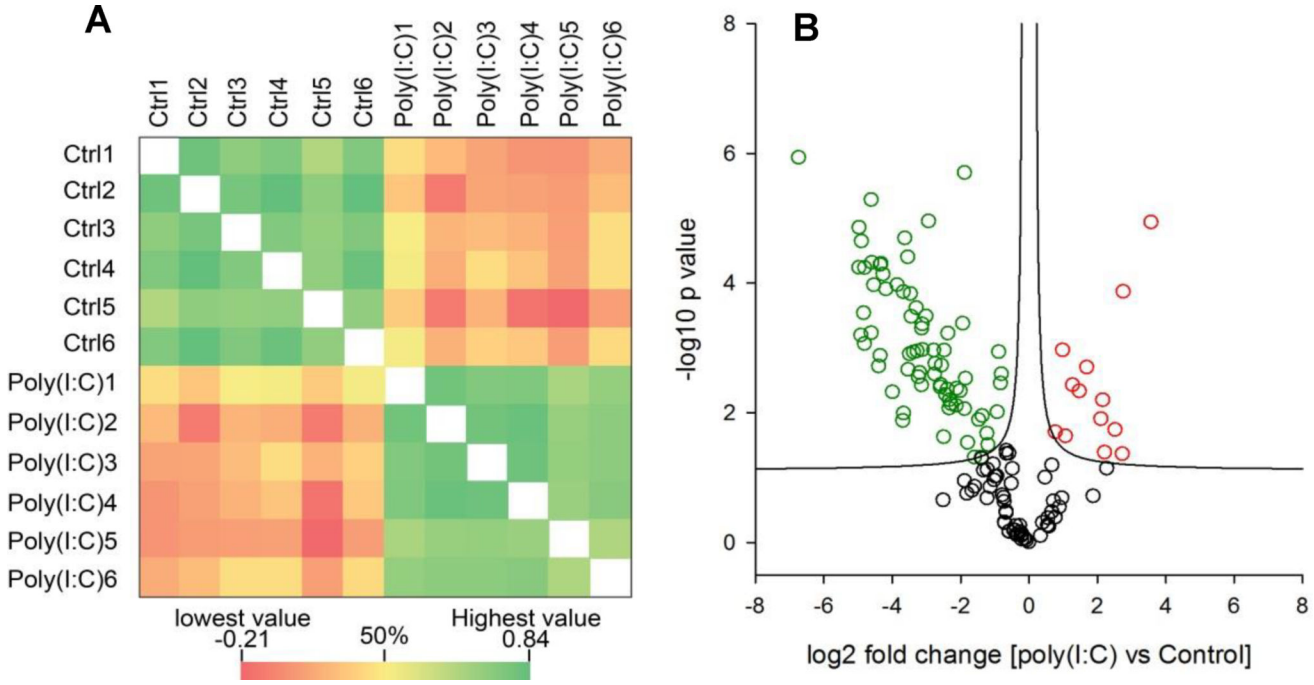

Figure 5.

Quantitative analysis of *in vivo* protein tyrosine nitration. The mice were administrated via intranasal with dsRNA [poly(I:C)]. The mice treated with PBS were used as control. The protein were extracted from the mouse lungs and digested with trypsin. The nitrotyrosine peptides were enriched with immunoaffinity purification and quantified with label-free approach. A total of 147 nitrotryrosine peptides were quantified. (A) The animal-to-animal Pearson correlation of expression level of 147 nitrotyrosine peptides. (B) Volcano plot for differentially expressed nitrotyrosine sites and by p value. Red circles, the nitrotyrosine sites up-regulated after poly(I:C) treatment; green circles, the nitrotyrosine sites down-regulated after ploy(I:C) treatment; the black circles, the nitrotyrosine sites were not significantly changed (Permutation FDR=0.01)

Author Manuscript Author Manuscript Author Manuscript Author Manuscript

Table 1

The nitrotyrosine-containing BSA peptides identified by LC-MS/MS analysis of tryptic digest of nitrated BSA (input) and the IP fraction (from anti-nitrotyrosine antibody enrichment).

Sequence	# of PSMs		Nitrotyrosine sites
	Input	IP	
MPCTEDYLSLILNR	12	7	Y7(Nitro)
DDPHACYSTVFDK	8	13	Y7(Nitro)
RPCFSALTPDETYVPK	10	6	Y13(Nitro)
DAFLGSFLYEYSR	2	2	Y11(Nitro)
ETYGDMADCCEK	3	20	Y3(Nitro)
EYEATLEECCAK	3	23	Y2(Nitro)
EYEATLEECCAKDDPHACYSTVFDK	0	1	Y2(Nitro)
GLVLIAFSQYLQQCPFDEHVK	1	0	Y10(Nitro)
HPEYAVSVLLR	1	5	Y4(Nitro)
HPYFYAPELLYYANK	0	10	Y11(Nitro)
HPYFYAPELLYYANK	0	8	Y11(Nitro); Y12(Nitro)
HPYFYAPELLYYANK	0	2	Y3(Nitro); Y5(Nitro); Y11(Nitro)
HPYFYAPELLYYANK	7	0	Y5(Nitro)
LGEYGFQNALIVR	0	4	Y4(Nitro)
RHPEYAVSVLLR	4	13	Y5(Nitro)
RHPYFYAPELLYYANK	0	1	Y6(Nitro); Y12(Nitro)
RHPYFYAPELLYYANK	1	0	Y6(Nitro)
YICDNQDTISSK	3	21	Y1(Nitro)
YIYEIAR	4	52	Y1(Nitro); Y3(Nitro)
YIYEIAR	38	236	Y3(Nitro) or Y1 (Nitro)
YNGVFQECCQAEDK	0	10	Y1(Nitro)

PSM, peptide spectrum match; IP, immunoprecipitation.